Recent results at HERA-B

Roberto Spighi (for the HERA-B collaboration)
INFN Sezione di Bologna
Via Irnerio, 46 - Bologna, Italy

Abstract

HERA-B is a fixed target experiment placed on the 920 GeV/c ($\sqrt{s} = 41.6$ GeV) HERA proton beam at DESY. During the last data taking period, 150 million dilepton triggers, 200 million minimum bias events and 35 million hard photon triggers were recorded.

The about 300.000 leptonic J/ψ decays acquired with the dilepton trigger are being exploited to study the direct production of charmonium mesons (J/ψ, $\psi(2S)$ and χ_c). Central subjects of this analysis are the Feynman-x (x_F) and transverse momentum (p_T) distributions, polarization and nuclear dependence of J/ψ and $\psi(2S)$, and the $\psi(2S)$ to J/ψ and χ_c to J/ψ production ratios. These measurements extend for the first time significantly into the negative-x_F region, which is of particular interest for the study of the peculiarities of charmonium production in proton-nucleus collision.

Measurements of the inclusive b-hadron and Υ cross sections are also performed using the dilepton sample. The inclusive production of D mesons and that of hard photons are among the remaining topics covered by the ongoing analyses, while already published results are a new limit on the branching ratio of the rare decay $D^0 \to \mu^+\mu^-$ and constraints on the production of pentaquark states.

1 Introduction

HERA-B is currently addressing a wide panorama of physics topics, ranging from strange, charmed and beauty hadron production to hard photon studies and pentaquark searches. Thanks to the large amount of statistics acquired during the last data taking period and to the use of different nuclear targets, these measurements are expected to result in a more complete and precise experimental picture of the inclusive hadronic production in proton-nucleus collisions with respect to the present situation. Moreover, the large acceptance of the detector allows to extend the kinematical range into the region of negative longitudinal momentum fraction x_F more than that of any other previous fixed-target experiment. Such an improvement is crucial for an extensive verification of perturbative QCD predictions over the widest possible range of processes, kinematical configurations and production energies. The particular environment in which these processes are studied in a fixed target experiment constitutes by itself an additional reason of interest: the investigation of the peculiarities of hadronic production in nuclear matter extends its scope up to the frontier with a topical subject like the quark-gluon plasma.

One of the most sensitive probes of the properties of nuclear matter is the production of charmonium from nuclear targets [1]. Measurements of the charmonium production cross sections (J/ψ, $\psi(2S)$ and χ_c) in proton-nucleus (pA) collisions are important as a test of many different models attempting to describe the nuclear modification of inclusive single-particle productions, which still needs experimental confirmation. Such models complement the basic colour singlet and colour octet mechanisms [2] of quarkonium production with the inclusion of processes accounting for the effects of interaction with the nuclear matter, like final state absorption, interactions with comovers, shadowing of parton distributions, intrinsic heavy quark components and parton energy loss [3]. The understanding of the mechanisms of particle production induced by pA collisions in the presence of an ordinary, confined nuclear state is crucial for the correct interpretation of the recent measurement of suppressed J/ψ production in Pb-Pb collisions performed by the NA50 collaboration [4], for which there is not yet a general consensus as to whether it represents an evidence of quark-gluon plasma formation or can be explained as an ordinary effect of scattering from confined nuclear matter [5]. HERA-B is studying the production of J/ψ and $\psi(2S)$ as a function of the variables x_F, p_T of the decaying meson and of the cosine of the lepton decay angle $\cos\vartheta$, whose non-uniform distribution would indicate a polarization of the produced state. Improvements with respect to the previous experimental situation are represented by the high energy of the experiment (the highest among the fixed-target ones), the wide kinematical acceptance, covering negative x_F values, and the determination of the nuclear dependence in this region.

Other inclusive production studies which are being performed by HERA-B as independent sources of baseline information for the investigation of the quark-gluon plasma state are the measurements of strange and hyperon cross sections, for which the experiment can count on a sample of 200 million minimum bias events.

The program of measurements devoted to the verification of perturbative QCD includes, besides the already mentioned charmonium studies, also the hadronic productions of bottonium, open beauty, open charm and direct photons. Counting on comparable or larger statistics and wider or significantly different kinematical acceptances than the previous experiments, HERA-B can give a valuable contribution to the not particularly ample and sometimes unclear experimental situation. Hard photon data, in particular, besides representing one of the cleanest tests of perturbative QCD, can eventually lead to the first direct measurement of the gluon density function of the nucleon. The ongoing hard photon analysis, based on a sample of 35 million events acquired with a dedicated trigger and four different target materials, will provide the first nucleus-dependent measurement, which can be crucial in explaining the existing discrepancy between fixed-target measurements and the QCD predictions.

The big statistics of events acquired by HERA-B in the last data taking has made it possible to provide competitive results also in fields not directly related to the main physics program, such as, for example, the search for new hadronic states (pentaquarks) and the verification of Standard Model predictions (the decay $D^0 \to \mu^+\mu^-$). The pentaquarks are baryonic structures with at least five constituent quarks, whose existence is in principle allowed by QCD. Recent experimental results have shown evidences of their production in high energy collisions. HERA-B has performed a search of the $\Theta^+(1540)$ and $\Xi^{--}(1862)$ states, based on 200 million minimum bias events, providing limits to their production which are somehow at variance with the results of other experiments. The flavour-changing neutral current (FCNC) decay $D^0 \to \mu^+\mu^-$ is strongly suppressed in the Standard Model (SM), which predicts a branching ratio of the order 10^{-19}, well below the sensitivity of the current experiments. However, in the extensions of the SM the predicted value can be enhanced by several orders of magnitude. A new experimental constraint published by HERA-B already intersects the range of values (up to $\approx 10^{-6}$) allowed in the Minimal Supersymmetric Standard Model.

The following sections give an overview of the physics analyses here briefly introduced; results obtained by HERA-B, mostly in a still preliminary form, are presented and compared with the experimental situation. The description of the measurements is preceded, in the next section, by a brief account of the characteristics of the detector and of the acquired data samples.

2 Apparatus and data taking

HERA-B is a fixed target experiment installed at the HERA accelerator, operating with protons of 920 GeV/c momentum against nuclear targets. The spectrometer has a wide forward geometry, covering up to 220 mrad in the bending plane and 160 mrad in the vertical plane. The high angular coverage allows to investigate kinematic regions (for example the negative-x_F range in the J/ψ or $\psi(2S)$ analyses) not accessible in previous high energy experiments. A side view of the detector is shown in Fig. 1.

HERA-B is composed by a target, a silicon vertex detector (VDS), a magnet, a tracking system, a ring imaging Cerenkov hodoscope (RICH), an electromagnetic calorimeter (ECAL) and a muon detector (MUON). A complete description of the apparatus is given elsewhere [7]; here only the characteristics which are essential for a general understanding of the measurements are recalled.

The target setup [8] consists of 2 stations separated longitudinally by 4 cm along the beam line. Each station contains four wires of different materials (C, Al, Pd, W, Ti), each having a size of 50 - 100 μm perpendicular to the beam and 0.5 - 1 mm along the beam. They can be remotely and individually moved inside the beam halo, in order to adjust the interaction rate. The data acquisition was performed with a maximum of two targets inserted simultaneously and a total interaction rate varying from 5 to 10 MHz.

The VDS [9] consists of 7 stations of double-sided silicon strip modules, with dimensions 50 $\times$ 70 mm^2 and 50 μm pitch. The stations are integrated on a movable Roman pot system inside the vacuum vessel and can be placed as near as 10 mm to the beam. The VDS allows a vertex resolution of 50 and 450 μm respectively in the transverse (x,y) and parallel (z) directions with respect to the proton beam.

A dipole magnet of 2.13 Tm field integral houses a first set of Main Tracker stations, followed by a second set of large tracking devices extending up to 13 m downstream of the interaction region.

Given the large gradient of particle flux with increasing distance to the beam, the tracking system is divided into the so called Inner Tracker (ITR) and outer Tracker (OTR) subsystems. The ITR [10],

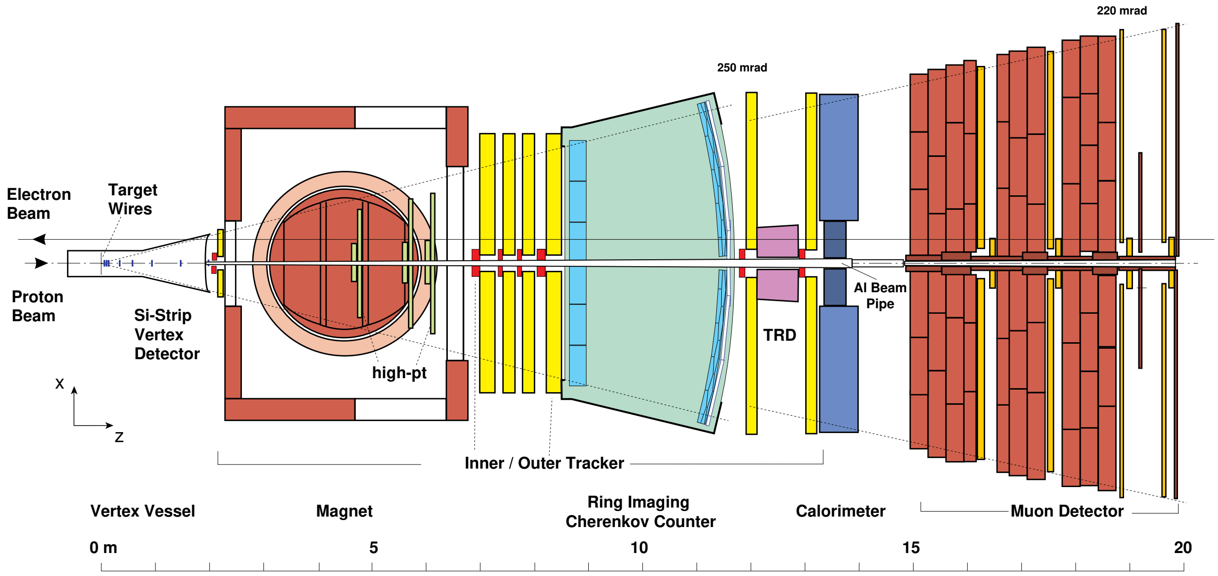

Figure 1: Side view of the HERA-B detector.

Table 1: ECAL spatial and energy resolutions

	INNER	MIDDLE	OUTER
σ_E/E (%)	$20.5/\sqrt{(E)} \oplus 1.2$	$11.8/\sqrt{(E)} \oplus 1.4$	$10.8/\sqrt{(E)}$
σ_X (cm)	$1.25/\sqrt{(E)} \oplus 0.02$	$1.37/\sqrt{(E)} \oplus 0.28$	$2.17/\sqrt{(E)} \oplus 0.28$

which covers the inner angular range of the acceptance (≤ 20 mrad), was not used in the last data taking. The OTR [11] is built of honeycomb drift chambers, with wire pitches of 5 mm in the region closer to the beam and 10 mm outside. The detector reached a hit efficiency of about 98% for the 10 mm chambers and about 95% for the 5 mm ones. The first station of the tracking system is placed upstream of the magnet and the remaining 6 stations extend from the downstream end of the magnet to ECAL.

The particle identification (PID) is performed by the RICH [12], the ECAL [13] and the MUON [14].

The RICH consists of a C_4F_{10} radiator volume with a longitudinal dimension of 2.5 m and a photo multiplier plane collecting the light emitted by the charged particles. It allows π/K and a K/p separation respectively in the momentum ranges of $[10 \div 60]$ GeV$/c$ and $[20 \div 100]$ GeV$/c$.

The ECAL is based on a shashlik sampling calorimeter technology, with Pb and W absorbers sandwiched between scintillator layers. It is composed of three different lateral sections (Inner, Middle and Outer), each having a specific granularity adjusted to the occupancy gradient. The ECAL is used both to initiate trigger seeds in the electron channel and for data reconstruction. The performance of the calorimeter regarding the energy and spatial resolution are summarized in table 1.

The MUON system consists of 4 tracking stations located in the most downstream portion of the detector, at different depths in iron loaded absorbers. It is composed of two different technologies, with gas pixel chambers in the inner most region and conventional tube chambers in the outer section. As in the case of the electromagnetic calorimeter, the MUON is used both at trigger level (for the muon channel) and for the reconstruction.

The data acquisition was performed in two different periods: the first one, during the year 2000, mainly dedicated to the debugging of the apparatus and the second one, from October 2002 to March 2003, for the physical analyses.

The last data taking has been performed using three different trigger configurations: minimum bias

(MB), dilepton and hard photon. The MB trigger requires at least one proton target interaction with the presence of deposited energy in the RICH detector. The dilepton trigger has been implemented in order to select those particles that decay in two leptons (e^+e^- or $\mu^+\mu^-$). For this purpose the trigger has been designed in three different levels: pretrigger, First Level Trigger (FLT [15]) and Second Level Trigger (SLT [16]). The pretrigger asks for the presence of at least two clusters in the ECAL (for e^+e^-) or in the MUON (for $\mu^+\mu^-$) with a defined p_T threshold. Starting from the pretrigger coordinates, the FLT searches for tracks of charged particles in the MUON tracking layers (only for the $\mu^+\mu^-$ couples) and in four of the main tracker stations (OTR only). The momentum of a candidate track is inferred by assuming that the track originates at the target wires and calculating the bending angle within the magnetic field. Triggered events are required to have at least one FLT track in coincidence with one seed. From the pretrigger and the FLT candidates, the SLT searches and reconstructs the tracks across the whole detector up to the VDS. Events with at least two fully reconstructed tracks and with a common vertex are triggered. At the end, the events passing the SLT are assembled and transferred to a fourth level farm (no third level algorithm is applied), where a fraction of the events is fully reconstructed online for monitoring purposes. No event selection is applied at the fourth level. The total suppression factor is about $50 \cdot 10^3$ allowing a final archive rate of about 100 Hz. By running the muon and the electron triggers in parallel it is possible to perform all the analyses in both leptonic channels, providing significant consistency checks of the results.

The hard photon trigger has been implemented by requiring at least one neutral cluster of high transverse energy (typically > 3 GeV/c) on ECAL.

The total data sample consists of 150 million dilepton triggered events, 210 million minimum bias (MB) and 35 million hard photon events. The physics topics addressed using this large amount of data include the production of charmed, beauty and strange particles, SM verification, hard photons and pentaquark searches.

3 Charmonium studies

Concerning the charmonium production, a detailed study of the properties of the J/ψ, $\psi(2S)$ and χ_c mesons is being performed. All three mesons are reconstructed both in the e^+e^- ("electron") and $\mu^+\mu^-$ ("muon") decay channels. The meson reconstruction begins with the selection of the tracks which pass the electron/muon trigger requests; in this phase a clone recognition algorithm is applied in order to remove fake tracks generated by a small misalignment between the different subdetectors. The momentum is evaluated from the bending induced by the magnet, with special corrections applied for the electrons due to their electromagnetic nature. In fact, it is necessary to take into account and recover the energy loss along the electron path due to bremsstrahlung (BR) emission, ionization or other processes. Moreover, the higher percentage of background in the electron decay sample with respect to the muons forces to use more selective cuts for the electron identification. This background is mainly composed by pions strongly interacting with the absorber material of ECAL and by hadrons overlapping with energetic neutral showers. The electron identification is based on requests on the E/p distribution (E is the electron energy measured by ECAL and p is its momentum measured by the tracking) and on the topologic characteristics of the electromagnetic cluster. The quantity E/p is peaked at 1 for the electrons, which release all their energy on ECAL, while it is distributed at lower values for pions. The requests on the cluster topology consists in an energy deposition concentrated in the central part of the cluster and having a radial symmetric distribution. Due to the lower background affecting the muon channel, the only request of two muon clusters in the MUON detector already provide a good selection criterion. With these selection cuts, in the last data taking about 300000 J/ψ are reconstructed in both decay channels (see fig. 2).

The study of the J/ψ production include the measurement of the differential distributions with respect to the transverse momentum (p_T) and Feynman-x (x_F) of the J/ψ and the lepton decay angle in the J/ψ rest frame (θ). The normalization of all the charmonium distributions is at the moment arbitrary.

Fig. 3a shows the p_T differential distribution of the J/ψ obtained with a subsample of the electron

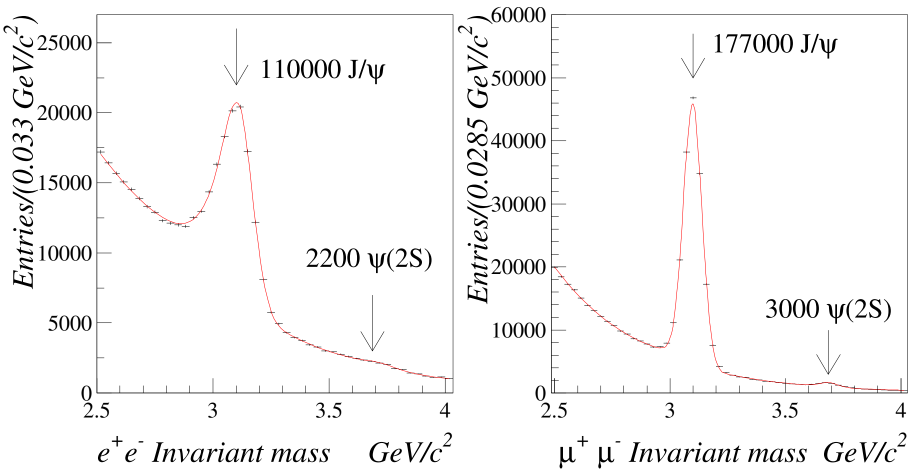

Figure 2: J/ψ peaks in the electron and muon channels.

Table 2: kinematic intervals and fitting parameters in measurements of the J/ψ differential distributions: preliminary HERA-B values compared to fixed-target results at $\sqrt{s} = 38.8$ GeV [17] (with statistical and systematic uncertainties combined).

exp.	target (A)	p_T range	$\langle p_T \rangle$ [GeV/c]	x_F range	c	λ
HERA-B	C (12)	< 4.5 GeV/c	1.24 ± 0.01	$-0.35 \div 0.10$	$5 \div 6.5$	$-0.5 \div 0.1$
	W (184)	< 4.5 GeV/c	1.29 ± 0.01		$(\pm 0.2_{\rm stat})$	$(\pm 0.1_{\rm stat})$
E771	Si (28)	< 3.4 GeV/c	1.20 ± 0.01	$-0.05 \div 0.25$	6.54 ± 0.23	-0.09 ± 0.12
E789	Be (9)			$0.30 \div 0.95$	5.32 ± 0.05	
	Cu (64)			$0.30 \div 0.95$	5.21 ± 0.04	
	Au (197)	< 2.6 GeV/c	1.29 ± 0.01	$-0.035 \div 0.135$	4.91 ± 0.18	
E672/E706	Be (9)	< 3 GeV/c	1.22 ± 0.01	$0 \div 0.6$	6.18 ± 0.16	-0.11 ± 0.15
E866/NuSea	Cu (64)	< 4 GeV/c		$0.25 \div 0.95$		0.07 ± 0.08

data, fitted with the function:

$$\frac{dN(J/\psi\ )}{dp_T^2} = \kappa \cdot \left[1 + \left(\frac{35 \cdot \pi \cdot p_T}{256 \cdot < p_T\ \ >} \right)^2 \right]^{-6}, \tag{1}$$

where the normalization factor κ and $< p_T >$ (average p_T) are free parameters of the fit. The analysis is performed separately for the carbon and tungsten targets and for the two J/ψ decay channels. Table 2 contains a summary of very preliminary results obtained by HERA-B for the differential distributions, together with the result of the fixed target experiments which are closest in energy to HERA-B [17]. 9 Thanks to the high acquired statistics, the HERA-B result extends the knowledge of the J/ψ production to a wider p_T range than the previous published results. As already found by previous experiments, the HERA-B result confirms the tendency of an increasing $< p_T >$ for heavier targets.

Fig.3b shows a preliminary x_F distribution obtained with the electron data, fitted with the function:

$$\frac{dN(J/\psi\ )}{dx_F} = \kappa' \cdot (1 - |x_F|)^c, \tag{2}$$

where κ' is the normalization parameter and c the "slope" of the curve. The range of variation quoted in tab. 2 for c ($5 \div 6.5$) includes the spread of preliminary evaluation performed with different subsamples of the muon and electron data and for different target materials. The final distributions, obtained distinguishing between the different target materials, will be the first measurements in the negative

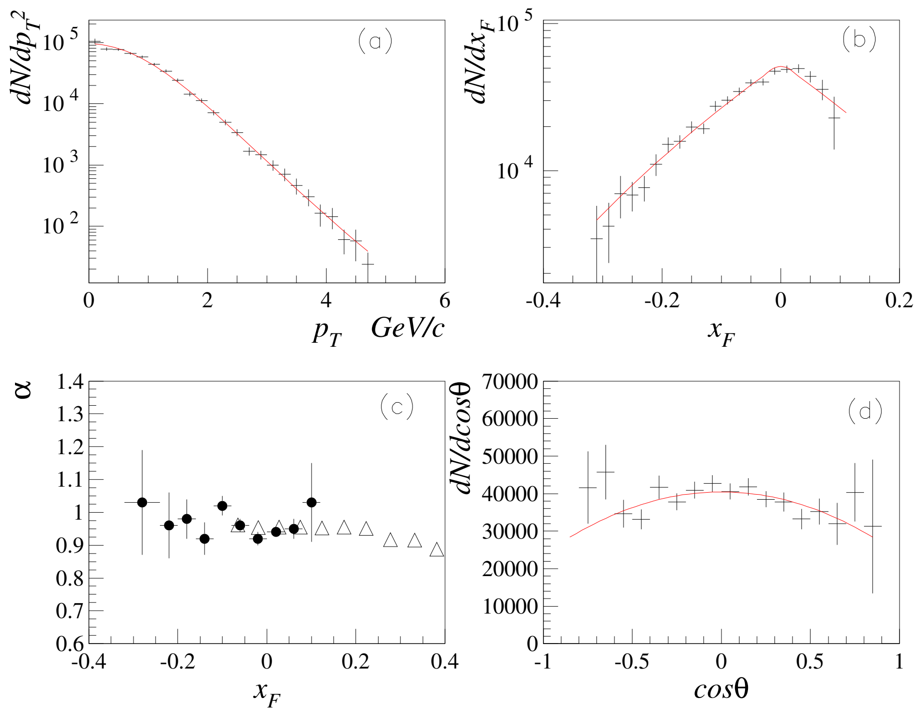

Figure 3: preliminary distributions of the J/ψ production as a function of p_T (a) and x_F (b). c) a very preliminary result (filled circles) for the suppression parameter α as a function of x_F compared with the measurement by E866 (empty triangle). d) preliminary distribution for the cosine of the lepton decay angle (θ) in the Gottfried-Jackson frame, from which the polarization parameter λ is extracted.

x_F range (see table 2), which is crucial for the study of the nuclear effects of the J/ψ production (A-dependence). A preliminary indication of the possibilities of this study is given by distribution shown in fig. 3c for the suppression parameter

$$\alpha = \frac{\ln(\sigma_{p\mathrm{W}}/\sigma_{p\mathrm{C}})}{\ln(A_{\mathrm{W}}/A_{\mathrm{C}})} \tag{3}$$

as a function of x_F (σ and A indicate respectively cross sections and target atomic weights). This preliminary analysis is based on data acquired with two target wires (C and W) simultaneously inserted into the beam, in order to minimize systematic uncertainties in the luminosity determination; a distribution obtained with a subsample of the muon data is compared in the figure with the result of the E866 experiment. The peculiarity of the HERA-B measurement, which covers for the first time a significant portion of the negative x_F spectrum, is made evident by the comparison. This study is important for the verification of different predictions of the models of nuclear suppression [18].

For the determination of the J/ψ polarization, the distribution of the variable $\cos\vartheta$, defined in the Gottfried-Jackson frame, is fitted with the function

$$\frac{dN(J/\psi\ )}{dcos\theta} = \kappa'' \cdot (1 + \lambda \cdot cos^2\theta), \tag{4}$$

where κ'' is a normalization factor and λ is the polarization parameter. $\lambda = 0(1, -1)$ means no (transverse, longitudinal) J/ψ polarization. A preliminary result based on about 15% of the total electron statistics is shown in fig. 3d. The range of variation $-0.5 < \lambda < 0.1$, obtained from the spread of preliminary results evaluated with different targets, indicates a preference for longitudinal rather that transversal polarization. The results obtained by previous experiments in different kinematical ranges (see table 2)

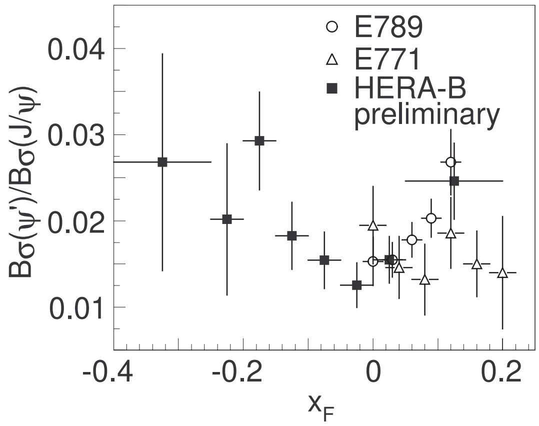

Figure 4: the $\psi(2S)$ to J/ψ yield ratio as a function of x_F, in a comparison with previous results.

are compatible with zero polarization. The final analysis will also include the evaluation of dependence of the polarization on the variables p_T and x_F.

The comparison between $\psi(2S)$ and J/ψ production can further contribute to the understanding of nuclear absorbtion processes: different cross section behaviours of the two charmonium states may in fact be interpreted in terms of the bigger size and lower binding energy of the $\psi(2S)$ with respect to the otherwise very similar J/ψ state. Preliminary results extracted from the e^+e^- sample are the yield ratio $\mathcal{B}(\psi(2S) \to e^+e^-)\sigma(\psi(2S))/\mathcal{B}(J/\psi \to e^+e^-)\sigma(J/\psi)$ for carbon ($0.016 \pm 0.002_{\text{stat}}$) and tungsten targets ($0.018 \pm 0.004_{\text{stat}}$). These values are in agreement with the world average value of about 0.016 and with the apparent independence of the target atomic weight and of the production energy shown by previous results. The $\psi(2S)$ to J/ψ ratio is also measured as a function of x_F, p_T and $\cos\vartheta$. The importance of the contribution of HERA-B in the current experimental panorama (limited to measurements by E771 and E789 [17] extending only in the positive x_F region) is made evident in Fig. 4.

The χ_c production has been studied measuring the fraction R_{χ_c} of J/ψ's produced via radiative χ_c decays. The χ_c has been detected in the decay channel $J/\psi\gamma$ with the $J/\psi \to \mu\mu$ (the analysis on the electron decay channel is ongoing). On the three different χ_c states, the χ_{c0} contribution has been neglected due to its small radiative branching ratio decay $(6.6 \pm 1.8) \cdot 10^{-3}$ [19]. The χ_{c1} and χ_{c2} states, with radiative branching ratios of 0.316 ± 0.033 and 0.202 ± 0.017 [20] respectively, are separated by 46 MeV/c^2; in most experiments the energy resolution is insufficient to resolve these two states, so usually the ratio between the sum of the production of all χ_c states with respect to the J/ψ is quoted. Fig. 5 shows the $J/\psi\gamma$ invariant mass referring on the 15% of the total muon data. The number of χ_c expected from the full data sample is $\simeq$ 15k which means an increasing statistics of about a factor of 20 with respect the first analysis published [21] by HERA-B with the previous data taking. A preliminary results gives $R_{\chi_c} = 0.21 \pm 0.05_{stat}$, in agreement with the $R_{\chi_c} = 0.32 \pm 0.06_{stat} \pm 0.04_{syst}$ already published. These results favour the NRQCD expectation [21], but more stringent tests and better precision are needed for a final conclusion.

4 Beauty studies

The beauty production was studied with the measurement of the $b\bar{b}$ and the Υ cross-sections relative to the J/ψ production.

The prediction on the $b\bar{b}$ cross section based on perturbative QCD [22] are compatible with experimental results from pion and proton beams, but both theoretical and experimental uncertainties are large. Only two measurements of the $b\bar{b}$ production cross section in $p - Nucleus$ interactions were previously reported [23]. The b-hadrons are detected in the inclusive channels $J/\psi X$ and are distinguished from the large prompt J/ψ background by exploiting the detached vertex decay, thanks to the long b decay (length in the apparatus $\approx$ 8 mm) compared to the vertex accuracy. Additional cuts on the impact parameter of the lepton tracks with respect to the target and the primary vertex have been requested. The J/ψ

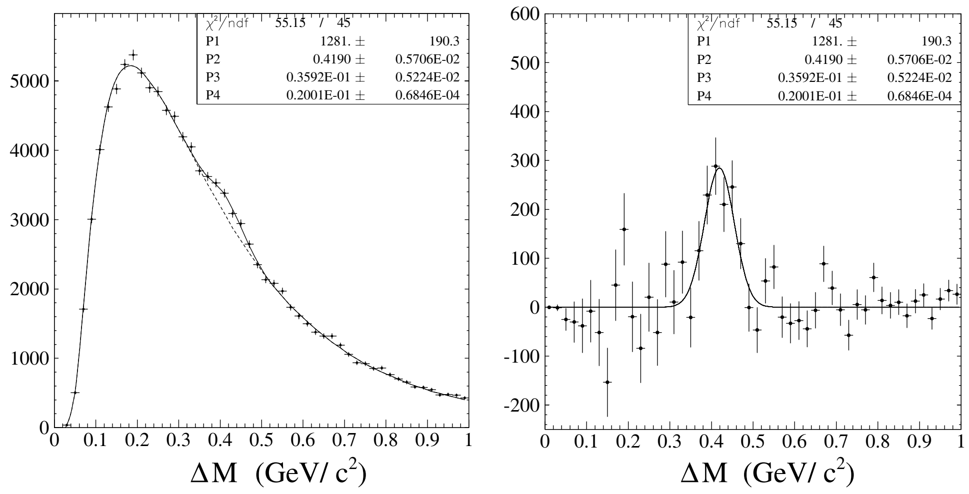

Figure 5: $J/\psi\gamma - J/\psi$ invariant mass (with the $J/\psi \to \mu^+\mu^-$) without and with background subtraction.

was detected in both $\mu^+\mu^-$ and $e+e^-$ decay channel in order to perform a combined $b\bar{b}$ production cross section measurement. In order to minimize the systematic error related to detector and trigger

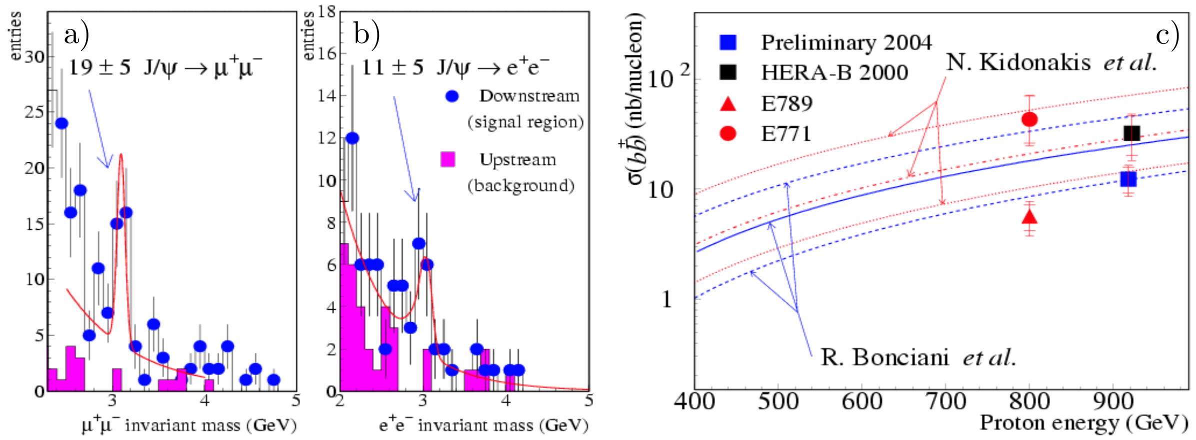

Figure 6: The J/ψ peaks for the detached events in the muon decay channel (a) and in the electron one (b) for the 35% of the total statistics. In (c), two different model predictions are plotted together to the experimental results.

efficiencies and to remove the dependence on the absolute luminosity determination, the measurements have been performed relative to the known prompt J/ψ production cross section [24]. In fig.6a-b, the J/ψ candidates having a detached decay vertex in the muon (electron) channel are shown for the 35% of the total statistics. The plots show about 20 and 10 candidate events in the muon and electron decay channel, respectively, corresponding to about 100 events for the full sample. The preliminary value is: $\sigma(b\bar{b}) = 12.3^{+3.5}_{-3.2}\ nb/N$ in agreement with the one obtained in a previous low statistic data taking [25]. These results are compared with the latest QCD calculations [22] beyond next to leading order (fig. 6c). The predicted values are in good agreement with the obtained measurements. In the same figure, the E789 and E771 experimental results [23] obtained with 800 GeV proton interactions on Au and Si, respectively, are plotted.

The production of hidden beauty was studied measuring the cross section of the Υ without distinction between the three states $\Upsilon(1S)$, $\Upsilon(2S)$ and $\Upsilon(3S)$. Many experiments evaluated the Υ production cross

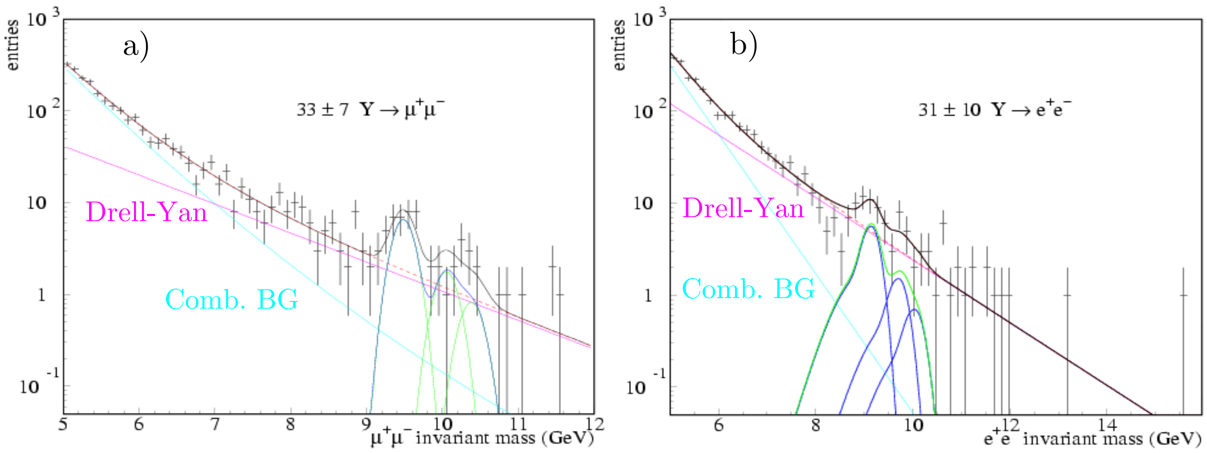

Figure 7: The Υ peaks in $\mu^+\mu^-$ (a) and $e+e^-$ (b) decay channel. The plots show also the different background contributions.

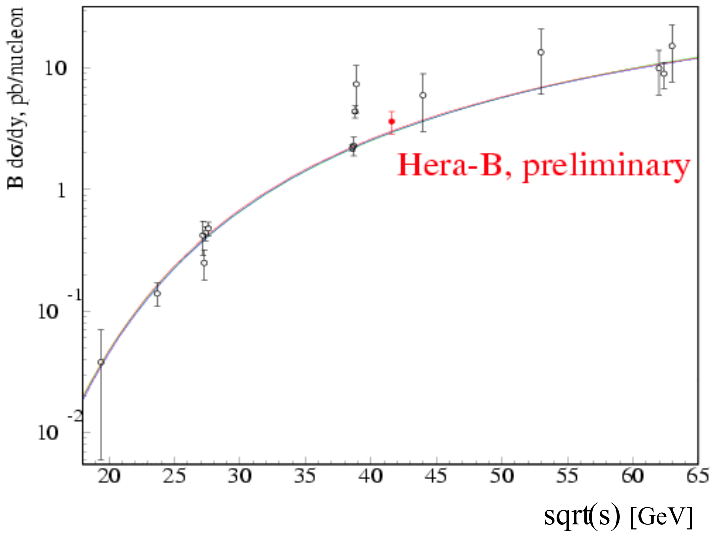

Figure 8: Data on the previous experiments on BR$\times$dσ/dy for Υ production, fitted with the Craigie parametrization

section, in a wide energy range ($\sqrt{s} = [19 - 1800]GeV$), with proton and pion beam and with different target materials [26]. In spite of this, the experimental panorama is not so clear especially in the energy region of HERA-B where the available results have a large disagreement. The Υ has been detected in both $\mu^+\mu^-$ and $e+e^-$ decay channel simultaneously in order to have a further consistency cross check; the fig.7 a-b shows the peaks of the three states partially resolved. The number of total reconstructed Υ resulted about 60, in particular 33 ± 7 in the muon channel and 31 ± 10 in the electron one. The cross section has been normalized to the J/ψ production and resulted in the preliminary values 3.9 ± 1.1 pb/N and 2.9 ± 1.2 pb/N respectively for $\mu^+\mu^-$ and $e+e^-$ decay channel; these values have been averaged to 3.4 ± 0.8 pb/N. The fig. 8 shows the agreement of the HERA-B result with respect the previous experimental measurements [27] as a function of the center of mass energy.

5 Hard photon studies

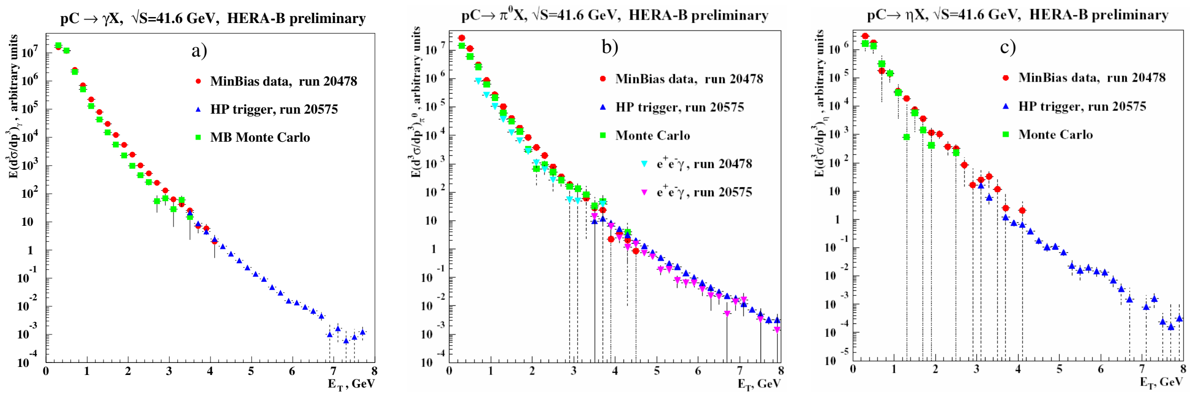

Figure 9: γ (a), π^o (b) and η (c) direct production in $p-C$ interactions with respect their transverse energy E_T.

The study of the production of the so-called *hard* or *prompt* photons is a sensitive probe of the mechanisms of hard scattering between nucleons and one of the cleanest stategies for the verification of QCD predictions. In fact, prompt photons are produced directly through a point-like coupling to the elementary constituents of the colliding nucleons and reach the detector with essentially unaltered kinematic characteristics. In particular, thanks to the dominant contribution of the Compton-like quark-gluon scattering $qg \to q\gamma$ in the production mechanism for high photon transverse energy, hard photon measurements offer an unique opportunity of determining the gluon density function of the nucleon directly, whereas the global fits to deep inelastic scattering data can provide, at present, only indirect determinations limited to small values of the fraction of nucleon momentum carried by the gluon. Unfortunately, in the present experimental situation the $p-$Be results obtained by E706 [31] at 530 and 800 GeV are in strong conflict with the NLO perturbative QCD predictions calculated for proton-proton collisions, indicating the necessity of investigating possible effects of nuclear dependence. This task is being accomplished by HERA-B, which can count on 35 million hard photon events collected with four different nuclear targets ($A = 12$ up to 184). The fig. 9 a-b-c shows preliminary spectra of the direct production of γ, π^o and η in $p-C$ interactions. This analysis will provide precise measurements of the differential cross sections of hard photon production, characterized by the highest energy and the largest E_T and rapidity acceptances among the fixed target experiments, and considered for the first time as a function of the target nucleus.

6 Inclusive charm and strange production

Among several inclusive production studies conducted by HERA-B on the minimum bias sample, measurements of open charm and strange cross sections have been performed. The D-meson production cross sections have been evaluated by reconstructing the signals $D^0 \to K^-\pi^+$, $D^+ \to K^-\pi^+\pi^+$ and $D^{\star+} \to D^0\pi^+$ (charge conjugates are here always implied). Figures 10 a-b-c show peaks containing, respectively, 189 ± 20 D^0's, 198 ± 12 D^+ and 43 ± 8 $D^{\star+}$. Preliminary numbers for the three cross sections, with statistical and systematic uncertainties, are $\sigma_{D^0} = 56.3 \pm 8.5 \pm 9.5$ μb/nucleon, $\sigma_{D^+} = 30.2 \pm 4.5 \pm 5.8$ μb/nucl and $\sigma_{D^{\star+}} = 27.8 \pm 5.2 \pm 3.9$ μb/nucl [32]. Fig. 11 shows the average of the first two cross sections together to the experimental panorama; the precision obtained by HERA-B is comparable or better than the previous measurements.

Another field, besides the already mentioned nuclear dependence studies, in which the experiment can contribute in establishing baseline measurements for comparison with nucleus-nucleus results, are

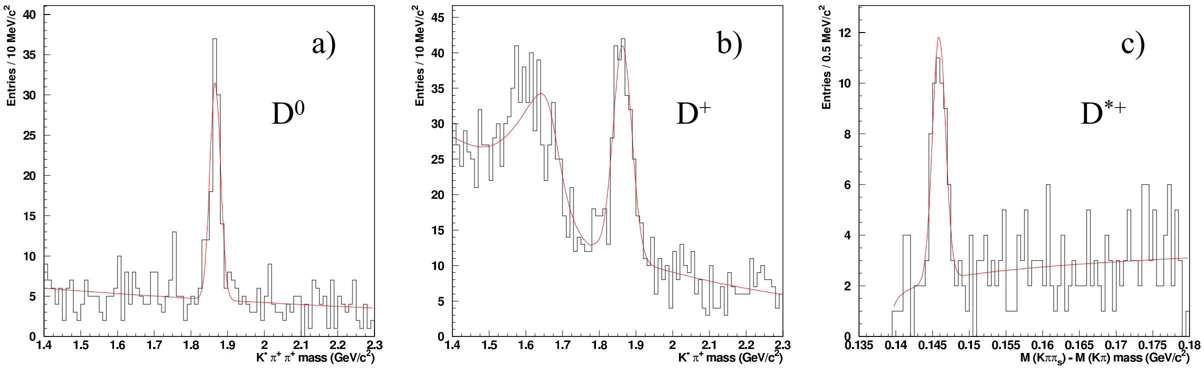

Figure 10: D^0, D^+ and $D^{\star +}$ peaks

.

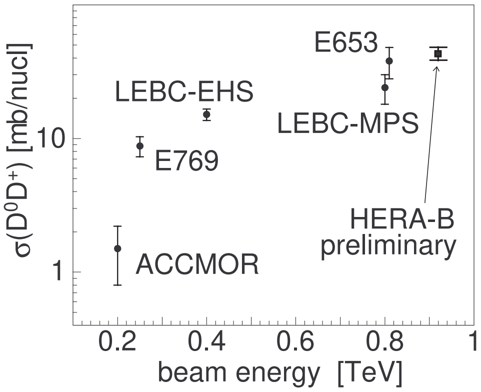

Figure 11: Preliminary result for $\sigma_{D^0 D^+} \equiv (\sigma_{D^0} + \sigma_{D^+})/2$ compared to the present experimental situation

.

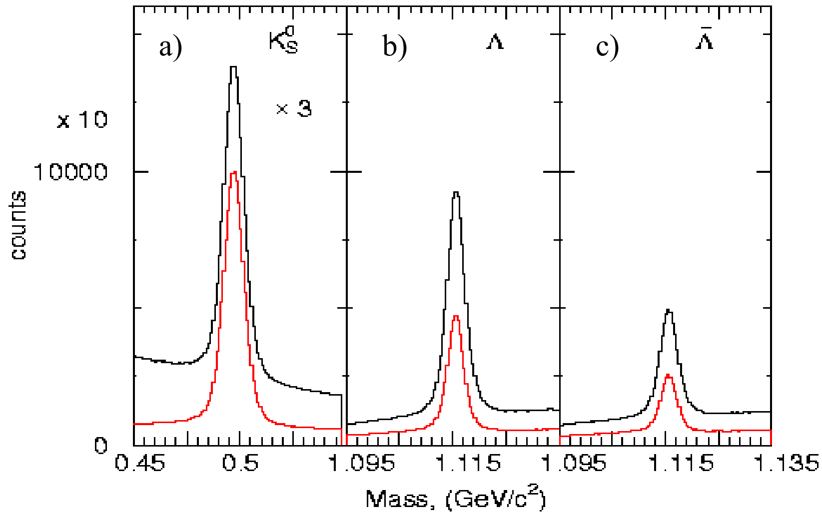

Figure 12: K_S (a), Λ (b) and $\overline{\Lambda}$ (c) peaks with and without the background subtraction.

the inclusive productions of strange particles (K^0_S, $K^\star$) and hyperons (Λ, $\overline{\Lambda}$), collectively referred to as V^0 particles. The production of strange particles is in fact expected to be enhanced in nucleus-nucleus collisions as a signature of the transition to the quark-gluon plasma state, while the antibaryon to baryon yield ratio at mid-rapidity and the shape of the p_T distributions of the V^0 particles can be related to the temperature of the nuclear system. With 3.4 million K_S, 940 thousand Λ and 450 thousand $\overline{\Lambda}$ acquired in the last data taking (see fig. 12), HERA-B is going to improve its measurements of inclusive production cross sections, nuclear dependence, p_T distributions and $\overline{\Lambda}/\Lambda$ yield ratios counting on a statistics 100 times higher than the results published with the 2000 data [33].

7 Pentaquark studies

One of the open problems inside the QCD is the possibility of the existence of non conventional particles as pentaquarks, $q\bar{q}q\bar{q}$ structures and glueballs. In the last years, the attention was polarized by several indications of exotic structures interpretated as pentaquarks (baryons with 4 quarks and 1 antiquark). HERA-B has investigated this field looking for the $\Theta^+(uudd\bar{s})$ and $\Xi^{--}(ddss\bar{u})$ candidates. On the basis of the chiral soliton model (CSM), the Θ^+ is expected to have a mass of 1530 MeV, a width of less than 15 MeV and to decay into a kaon and a nucleon [34]. In both the CSM and the correlated quark model [35], the Θ^+ is a member of an antidecuplet with two further exotic isospin 3/2 states of S=-2, the Ξ^{--} and the $\Xi^+_{3/2}$. Indications of the Ξ^{--} and its neutral isospin partner have been found in the $\Xi^-\pi^-$ and $\Xi^-\pi^+$ decay channels at a mass of 1862 MeV with a narrow width. The pentaquark search has been performed by selecting the Θ^+ and Ξ^{--} candidates in the decay channels pK_S and $\Xi^-\pi^-$ and charged coniugated (c.c.) respectively. The possibility to see the PQ candidates is based on the good identification of the K_S and $\Xi^- \to \Lambda\pi^-$ and c.c. (see fig. 12 or [36]). In figs. 13 and 14, the pK_S and $\Xi^-\pi^-$ (and c.c.) invariant masses are shown where no evidence for narrow Θ^+ and Ξ^{--} signals are visible, despite the fact that in the same plots or in similar analyses large signals of "normal" baryonic resonances are present (fig. 15).

The HERA-B results are summarized [37] by an upper limit on the following yield ratios (95% C.L.):

$$\Theta^+(1540)/\Lambda(1520) \quad < \quad 2.7\%, \tag{5}$$

$$\mathcal{B}\cdot\Xi^{--}_{3/2}(1862)/\Xi(1530)^0 \quad < \quad 4\%. \tag{6}$$

The corresponding absolute limits for the inclusive production cross sections at mid rapidity times the branching fractions are:

$$\mathcal{B}\cdot d\sigma(\Theta^+)/dy|_{y\approx 0} \quad < \quad 3.7\ \mu\mathrm{b/N}, \tag{7}$$

$$\mathcal{B}\cdot d\sigma(\Xi^{--})/dy|_{y\approx 0} \quad < \quad 2.5\ \mu\mathrm{b/N}. \tag{8}$$

8 $D^0 \to \mu^+\mu^-$

The branching ratio of the decay $D^0 \to \mu^+\mu^-$ is extremely sensitive to physics beyond the Standard Model. Experimental limits on its value provide a strong constraint on parameters of its possible extensions. Considering, as an example, a variant of Minimal Supersymmetric Standard Model with R-parity violation [28], the branching ratio can be enhanced from the unmeasurable 10^{-19} predicted by the Standard Model to a maximum allowed value of $3.5 \cdot 10^{-6}$. HERA-B has searched for this decay using about 50 million dimuon events. A set of general cuts on track parameters and transverse momentum of the (di)muon candidates has been defined to minimize the main background resulting from muon pairs produced by independent $\pi^\pm$ and $K^\pm$ decays, while maintaining a high efficiency for D^0 decays. Specific cuts on the separation between primary and secondary vertices, on the proper decay length and on the dimuon impact parameter to the primary vertex have then been used to isolate possible D^0 mesons, assuming that they are all produced directly at the target wire (at the production energy of HERA-B, the fraction of D^0 coming from B decays is less than 0.1%). The cut values are determined through a blind optimization procedure. After the selection, 31 dimuon events survive in the D^0 mass region, as shown in Fig. 16, where dashed and dotted lines separate the signal region from sideband background

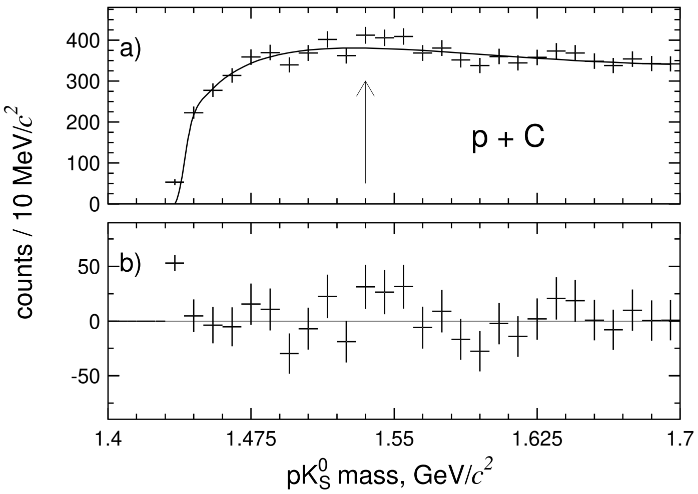

Figure 13: pK_S invariant mass. The arrow shows the position of the expected θ^+

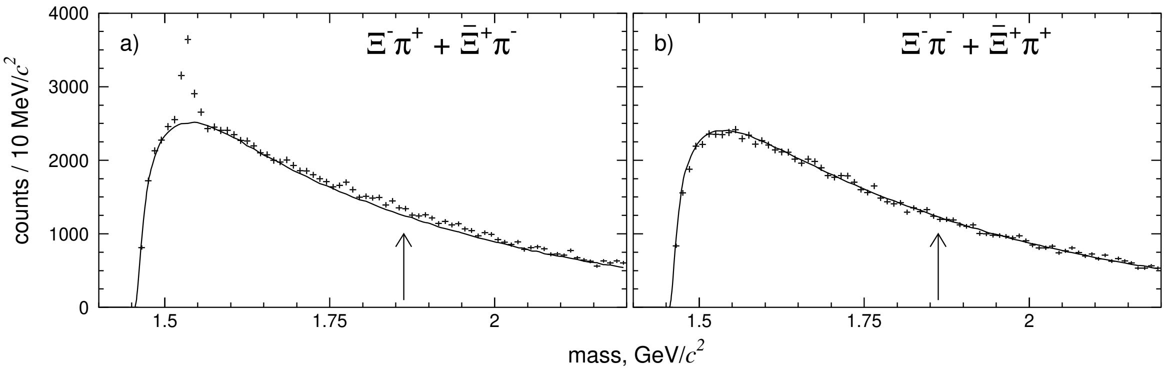

Figure 14: $\Xi^{\pm}\pi^{\mp}$ and $\Xi^{\pm}\pi^{\pm}$ invariant masses. Continuos lines show the background from event mixing. Arrows mark the mass of 1862 MeV/c^2. A clear signal of the $\Xi^o(1530)$ baryon is present, but no evidence of PQ candidates.

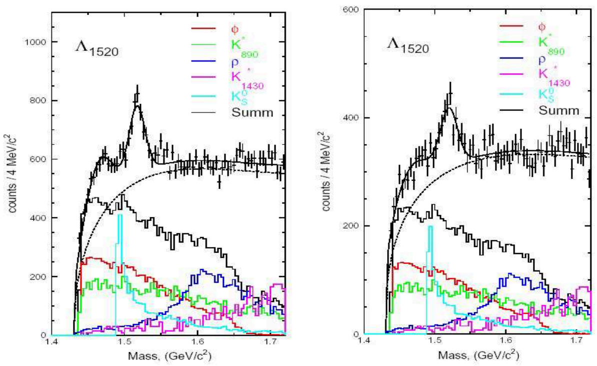

Figure 15: $\Lambda(1520)$ and $\bar{\Lambda}(1520)$ peaks with different background contributions

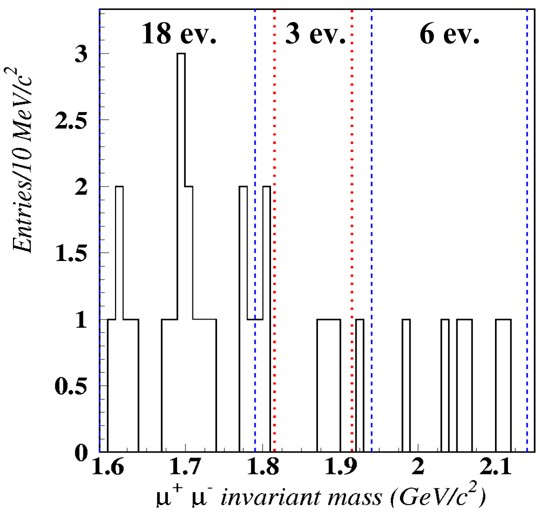

Figure 16: The dimuon mass spectrum in the D^0 region after the optimized selection cuts have been applied, with indication of the numbers of surviving events in the signal region and in the background sidebands.

regions. Using world average values of the ratio of D^0 to $J\psi$ production cross sections in proton-nucleus collisions, the three events in the signal region, compared to the extrapolated 6.0 ± 1.2 background events, are translated into an upper limit on the branching fraction of

$$\mathcal{B}(D^0 \to \mu^+\mu^-) \ < \ 2.0 \times 10^{-6} \tag{9}$$

at the 90% confidence level [29]. This results improves the previous best limit published by CDF [30].

9 Conclusions

A brief panorama of the studies performed at HERA-B has been presented. From OCTOBER 2002 to MARCH 2003, many millions of events have been acquired with different trigger types; the quality of the data is good allowing to investigate many physics fields as open and hidden production of strange, charm and beauty hadrons, studies on hard photons emission, FCNC processes and pentaquark search. Due to the high statistics many analyses have been performed using different nuclear targets for the investigation of the production processes. The high acceptance of the apparatus has permitted to obtain results in an extended range with respect the previous experimental panorama and its versatility has allowed the study the charmonium and the beauty production both in the electron and muon decay channel. A part of the presented results should be considered preliminary being the analysis still ongoing, while some are conclusive and already pubblished. The precision of the HERA-B results is in some case better or comparable with the previous experiments.

Acknowledgments

Many thanks to the conference organizers for the invitation and the logistic support.

References

[1] T. Matsui and H. Satz, Phys. Lett. **B178** (1986) 416

[2] P. Cho and A. Leibovich, Phys. Rev. **D53** (1996) 150;
M. Beneke and I.Z. Rothstein, Phys. Rev. **D54** (1996) 2005; **D54** (1996) 7082(E)

[3] R. Vogt, Phys. Rev. **C61** (2000) 035203

[4] M.C. Abreu *et al.* (NA50 Collaboration), Phys. Lett. **B499** (2001) 85

[5] A. Capella *et al.*, Phys. Lett. **B393** (1997) 431;
S. Gavin and R. Vogt, Phys. Rev. Lett. **78** (1997) 1006

[6] D.M. Jansen *et al.*, Phys. Rev. Lett. **74** (1995) 3118
T. Alexopoulos *et al.*, Phys. Rev. Lett. **82** (1999) 41
HERA-B Collaboration, I. Abt, et al., Eur. Phys. J. **CC26** (2003) 345

[7] HERA-B Collaboration, I. Abt, et al., Eur. Phys. J. **CC26** (2003) 091101

[8] K. Ehret et al., Nucl. Instr. Methods **A446** (2000) 190

[9] C. Bauer et al., Nucl. Instr. Methods **A501** (2003) 39

[10] W. Gradl, Nucl. Instr. Methods **A461** (2001) 80

[11] M. Hohlmann, Nucl. Instr. Methods **A461** (2001) 21

[12] M. Staric, Nucl. Instr. Methods **A502** (2003) 289

[13] G. Avoni et al., Nucl. Instr. Methods **A461** (2001) 332

[14] V. Eiges et al., Nucl. Instr. Methods **A461** (2001) 104

[15] V. Egorytchev et al., IEEE Trans. Nucl. Sci. **NS-50** (2003) 859

[16] P. Kreuzer et al., Nucl. Instr. Methods **A462** (2001) 212

[17] E789: M.S. Kowitt *et al.*, Phys. Rev. Lett. **72** (1994) 1318;
and M.H. Schub *et al.*, Phys. Rev. **D52** (1995) 1307;
E771: T. Alexopoulos *et al.*, Phys. Rev. **D55** (1997) 3927;
E672/E706: A. Gribushin *et al.*, Phys. Rev. **D62** (2000) 012001;
E866/NuSea: T.H. Chang *et al.*, Phys. Rev. Lett. **91** (2003) 211801

[18] R. Vogt, Nucl. Phys. **A700** (2002) 539.
K.G. Boreskov and A.B. Kaidalov, JETP Lett. **77** (2003) 599

[19] D.E. Groom *et al.*, Review of Particle Physics, Eur. Phys. J. **CC15** (2000) 1

[20] S. Eidelman *et al.*, Review of Particle Physics, Phys. Lett. **B592** (2004) 1

[21] HERA-B Collaboration, I. Abt, et al., Phys. Lett. **B561** (2003) 61

[22] P. Nason, QCD at High Energy, Proceeding of the XX International Symposium on Lepton and Photon Interactions at High Energy, hep-ph/0111024;
S. Frixione *et al.*, Adv. Ser. Direct. High Energy Phys. ˜**15** (1998) 609;
R. Bonciani *et al.*,Nucl. Phys. **B529** (1998) 424;
N. Kidonakis *et al.*,Phys. Rev. **D64** (2001) 114001

[23] D.M. Jansen *et al.*, Phys. Rev. Lett. **74** (1995) 3118;
T. Alexopoulos *et al.*, Phys. Rev. Lett. **82** (1999) 41

[24] M.H. Schub *et al.*, Phys. Rev. **D52** (1995) 1307;
T. Alexopoulos *et al.*, Phys. Rev. **D55** (1997) 3927

[25] HERA-B Collaboration, I. Abt, et al., Eur. Phys. J. **CC26** (2003) 345

[26] M. Grossman-Handschin *et al.*, Phys. Lett. **B179** (1986) 170;
NA3 collab., J.Badier *et al.*, Phys. Lett. **B86** (1979) 98;
J.K. Yoh *et al.*, Phys. Rev. Lett. **41** (1978) 684;
W.R. Innes *et al.*, Phys. Rev. Lett. **39** (1977) 1240;
K. Ueno *et al.*, Phys. Rev. Lett. **42** (1979) 486;
S. Childress *et al.*, Phys. Rev. Lett. **55** (1985) 1962;
E605 collab., G. Moreno *et al.*,Phys. Rev. **D43** (1991) 2815;
E605 collab., T. Yoshida *et al.*,Phys. Rev. **D39** (1989) 3516;
CCOR collab. Prooced. 1979 Int. Symp. on Lepton and Photon Interactions at High Energies, Fermilab, Illinois, USA, 1979, p. 232;
C. Kourkoumelis *et al.*, Phys. Lett. **B91** (1980) 481;
A.L.S. Angelis *et al.*, Phys. Lett. **B87** (1979) 398;
UA1 collab., C. Albajar *et al.*, Phys. Lett. **B186** (1987) 237;
E772 collab. D.M. Alde *et al.*, Phys. Rev. Lett. **64** (1990) 2479;
E772 collab. P.L. McGaughey *et al.*, Phys. Rev. **D50** (1994) 3038;
CDF collab. F. Abe *et al.*, Phys. Rev. Lett. **75** (1995) 4358;
E771 collab., T. Alexopoulos *et al.*, Phys. Lett. **B374** (1996) 271

[27] N.S. Craige, Phys.Rept. 47 (1978) 1;
G.A. Schuler, CERN-TH.7170/94; hep-ph/9403387.

[28] G. Burdman et al., Phys. Rev. **D66** (2002) 014009

[29] I. Abt et al., Phys. Lett. **B596** (2004) 173

[30] D. Acosta et al., Phys. Rev. **D68** (2003) 091101

[31] L. Apanasevich et al., Phys. Rev. Lett. **81** (1998) 2642

[32] A. Gorisek for the HERA-B collab. Prooced. 17th Int. Conf. on Ultra Relativistic Nucleus-Nucleus Collisions (Quark Matter 2004), Oakland, California, 2004, J.Phys.G30:S1163-S1166,2004.

[33] HERA-B Collaboration, I. Abt et al., Eur. Phys. J. **CC29** (2003) 181

[34] D. Diakonov et al., Z. Phys. **CA359** (11997) 305

[35] R. Jaffe et al., Phys. Rev. Lett. **91** (2003) 232003

[36] K.T. Knopfle for the HERA-B collab. Prooced. 17th Int. Conf. on Ultra Relativistic Nucleus-Nucleus Collisions (Quark Matter 2004), Oakland, California, 2004, J.Phys.G30:S1363-S1366,2004.

[37] HERA-B Collaboration, I. Abt et al., Phys. Rev. Lett. **93** (2004) 212003